Advances in development of Nb_3Sn superconducting radio-frequency cavities

Sam Posen* and Matthias Liepe

CLASSE, Cornell University, Ithaca, New York 14853, USA
(Received 6 July 2014; published 13 November 2014)

A 1.3 GHz Nb_3Sn superconducting radio-frequency cavity prepared with a modified annealing step reached $B_{pk} > 50$ mT, well above $B_{c1} = 25 \pm 7$ mT, without the strong Q-slope observed in previous Nb_3Sn cavities. At 4.2 K, it has a Q_0 of approximately 1×10^{10} at > 10 MV/m, far outperforming Nb at useable gradients. At 2 K, quench occurred at $\sim$55 mT, apparently due to a defect, so additional treatment may increase the maximum gradient. Material parameters of the coating were extracted from Q vs T data, including a T_c of 18.0 ± 0.1 K, close to the maximum literature value. High power pulses were used to reach fields far higher than in CW measurements, and near T_c, quench fields close to the superheating field were observed. Based on a review of previous experience with Nb_3Sn cavities, a speculative mechanism involving weak link grain boundaries is presented to explain how the modified annealing step could be the cause of the absence of strong Q-slope. Finally, an analysis of the progress to date provides hints that the path forward for Nb_3Sn cavities should focus on minimizing defects.

DOI: 10.1103/PhysRevSTAB.17.112001 PACS numbers: 74.70.Ad, 74.25.Op, 74.25.nn, 29.20.Ej

I. INTRODUCTION

Superconducting radio-frequency (SRF) researchers have been highly effective at finding preparation methods that suppress performance-limiting effects in niobium particle accelerator cavities. Now cavities are regularly produced that operate very close to the fundamental limits of niobium: they have surface resistances R_s very close to the ideal BCS value at operating temperatures, and they reach peak surface magnetic fields B_{pk} very close to the superheating field B_{sh}, the ultimate limit of the Meissner state [1]. To continue to keep up with continually increasing demands of future SRF facilities, researchers have begun a significant effort to develop alternative materials to niobium, materials with smaller BCS R_s and/or larger predicted B_{sh}.

Nb_3Sn is one of the most promising alternative SRF materials. Because it has a high critical temperature T_c of $\sim$18 K, compared to 9.2 K for niobium, its R_{BCS} at a given temperature is much smaller. This makes the material ideal for continuous wave (CW) linacs: benefits include a smaller and simpler cryogenic plant, the possibility of 4.2 K operation (no superfluid; atmospheric operation), and higher cost-optimum accelerating gradients E_{acc} in CW operation [2,3]. It has a large [4] thermodynamic critical field B_c, which in turn causes it to have a predicted B_{sh} of up to $\sim$400 mT (depending on the material parameters used for the calculation) [6] approximately twice that of Nb. This makes the material ideal also for high energy linacs: it would allow Nb_3Sn cavities to operate at higher accelerating gradients than Nb cavities, and therefore fewer cavities would be required.

Compared to niobium, only a small amount of research and development has been dedicated to Nb_3Sn for SRF applications, but research projects by several labs have made considerable progress with the material, starting in the 1970s. Pioneering work was done by Siemens AG [7], Kernforschungzentrum Karlsruhe [8], University of Wuppertal [9], Cornell University [10], Jefferson Lab [11], CERN [12], and SLAC [13].

Siemens researchers demonstrated the high gradient potential of Nb_3Sn coatings, achieving very high surface magnetic fields—even at 4.2 K—in 10 GHz cavities. R_s values were in the $\mu\Omega$ range, which is expected at this frequency due to the $R_s \sim f^2$ dependence of the BCS resistance. Results of several different high performing cavities given somewhat different preparations are summarized in Fig. 1 (for ease of comparison, the R_s shown is the weighted average given by G/Q_0, where G is the geometry factor of the cavity and Q_0 is the intrinsic quality factor).

Researchers at the University of Wuppertal obtained very small R_s values in Nb_3Sn cavities with shapes and frequencies appropriate for particle accelerators. At 2.0 K and at 4.2 K, at small accelerating gradients, they measured R_s values far lower than would be achieved by an uncoated Nb cavity; however, their cavities showed strong Q-slope (increasing R_s with B_{pk}). The graph of quality factor Q_0 vs accelerating gradient E_{acc} of one of the best cavities produced by University of Wuppertal is shown in

*sep93@cornell.edu

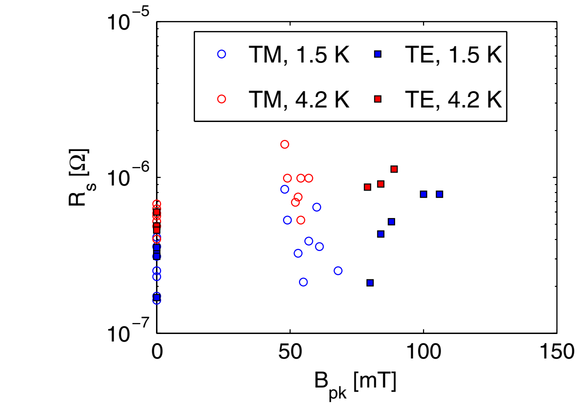

FIG. 1. 1.5 K and 4.2 K data for some of the best Nb_3Sn TM and TE 10 GHz cavities produced by Siemens AG [14,15]. Only the Q_0 at zero field and at the maximum field were reported. Due to the f^2 dependence of the BCS resistance, R_s values here correspond to the nΩ range at ~1 GHz.

Fig. 2 [16]. It is a 1.5 GHz single-cell cavity of the CEBAF shape that was tested at Jefferson Lab. Neither field emission nor quench was observed in this measurement; the limitation was available rf power.

In a later study, Wuppertal and JLab researchers tested three Nb_3Sn cavities, each of which exhibited strong Q-slope above an onset field, similar to Fig. 2. They used temperature mapping to study the distribution of heating over the surfaces. Though somewhat limited by saturation effects, they observed increased heating over broad regions after the onset of Q-slope consistent with the increased losses. They also observed a trend: a similar onset field for the strong Q-slope and increased heating in their cavities. Moreover, this onset field fell within the expected range for the lower critical field B_{c1} of Nb_3Sn. This led to speculation that the Q-slope was caused by a fundamental loss mechanism that occurred above B_{c1}, such as bulk vortex dissipation [17,18]. If strong losses above B_{c1} were unavoidable, then not just Nb_3Sn, but bulk alternative SRF materials in general—which tend to have relatively small B_{c1} values—would be severely limited.

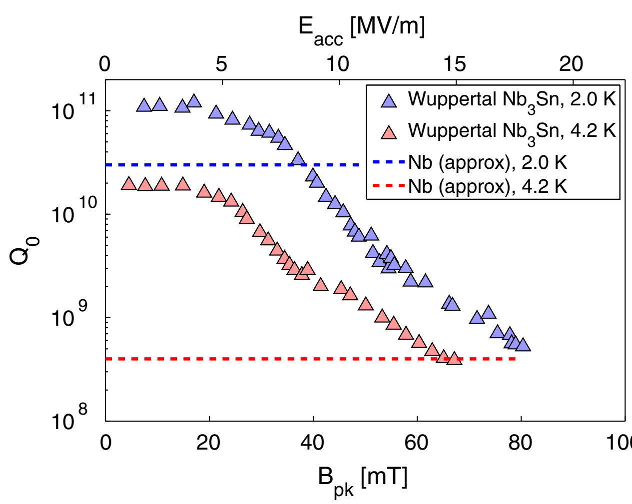

FIG. 2. Performance curves at 2.0 K and 4.2 K for one of the best Nb_3Sn cavities produced by U. Wuppertal [16]. The approximate values that could be expected for an equivalent Nb cavity are shown for comparison.

Researchers at the University of Wuppertal continued their investigations of Nb_3Sn, measuring films prepared on 1" diameter samples rather than full cavities. By varying the thickness of the films, they could control the grain size, and perform a systematic study of its effect on maximum sustainable rf field by testing their films in a 19 GHz resonator. They interpreted their results as showing a competition between two effects. At grain sizes above ~1.5 μm, they found that the field limitation could be explained by local thermal overheating. At smaller grain sizes, their analysis implicated weak link behavior as the cause for strong Q-slope, in which grain boundary regions would be driven normal conducting above a critical current [19].

II. Nb_3Sn CAVITY PREPARATION AT CORNELL

Nb_3Sn development at Cornell began in 2009 with the design, fabrication, and commissioning of a small coating chamber for samples. After establishing the capability to repeatedly produce Nb_3Sn films of sufficiently high quality for cavity rf surfaces [20], researchers constructed a larger chamber, for coating single cell 1.3 GHz cavities, shown in Fig. 3. The coating procedure was based on the vapor diffusion recipe developed by Wuppertal [11,21]. It involves placing a niobium cavity into a UHV furnace with a tin source, a $SnCl_2$ source, and niobium witness samples for surface analysis. The furnace temperature is raised to about 500 °C, where the $SnCl_2$ nucleates tin sites on the surface, then coating occurs at about 1100 °C, with the tin source temperature slightly elevated to about 1200 °C. After approximately 3 hours of coating, the tin source heater is shut off—this is done first to give excess tin

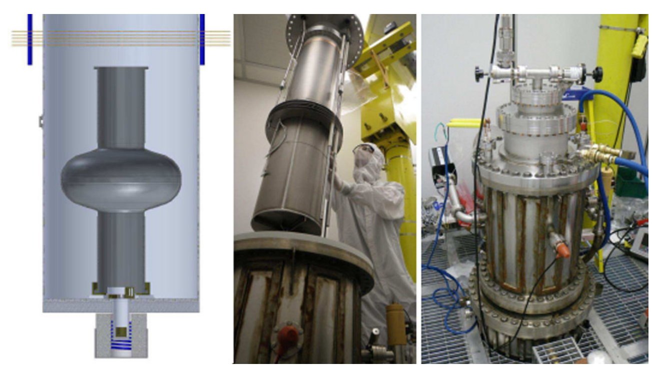

FIG. 3. Cross section of coating chamber (left), coating chamber being lowered into furnace (center), and UHV furnace with chamber inside (right).

FIG. 4. Coated cavity (left); view looking down into cavity before (top right) and after coating (bottom right).

time to diffuse—then after 30 minutes, the furnace is turned off.

Visually, the Nb_3Sn surface is a darker gray than niobium, and it is matte rather than shiny, as shown in Fig. 4. The thickness of the coating can be measured by cutting into a witness sample using a focused ion beam (FIB), then taking images of the exposed cross section. The Nb_3Sn layer produced using this technique is approximately 1–3 μm thick. A FIB cross section of a witness sample is shown in Fig. 5.

Two cavities have been coated to date, both with Cornell Energy Recovery Linac (ERL) shape [22] (similar to TESLA [23]), and both made from RRR ~300 niobium. Cavity A was prepared as described above, a method that shall be referred to as preparation A. For cavity B, a modification was made to Wuppertal's recipe: after the tin source heater was shut off, the cavity was annealed at about 1100 °C for approximately 6.5 hours before turning off the furnace instead of for just 30 minutes. The method with the extra long annealing step will be referred to as preparation B.

The witness samples were studied under scanning electron microscope (SEM), and images from both

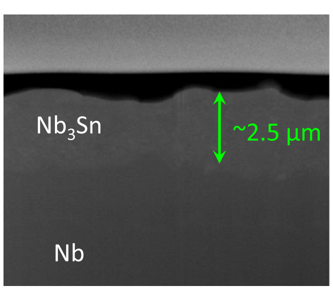

FIG. 5. Cross section near the surface of a witness sample.

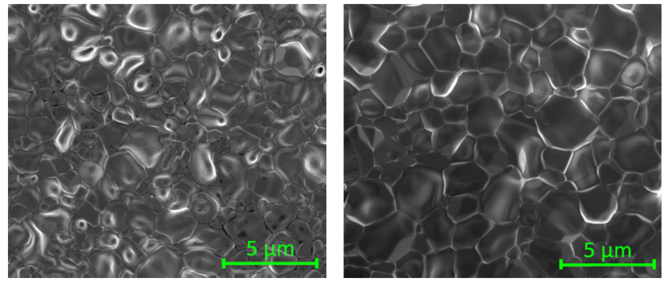

FIG. 6. SEM images of witness samples coated using preparations A (left) and B (right).

preparations can be seen in Fig. 6. Preparation B, which involved leaving the substrate at high temperatures for longer, resulted in larger Nb_3Sn grains. By inspection, the grains for preparation A are ~1 μm in size, whereas those from preparation B are ~2 μm in size. The images were analyzed to determine the approximate number of grain boundaries per unit length. Respectively, this resulted in 1.6 ± 0.2 and 0.8 ± 0.1 grain boundaries per μm for preparations A and B.

After coating, both cavities were treated with only a high pressure rinse (HPR) before mounting to a vertical test stand for CW cryogenic performance test. Before insertion to the dewar, the outside cavity surface was covered with an array of temperature sensors (temperature map) to obtain information about the loss distribution [24]. The temperature map consists of 38 boards, each with 17 sensors. The cavity was cooled at a very slow rate, $\gtrsim 6$ min/K, as specified by Wuppertal researchers, to minimize trapped flux due to thermocurrents [5].

Following CW testing, cavity B was tested in pulsed mode with up to 1 MW of power from a klystron. Pulsed power was used to reach high fields in the cavity very quickly (<100 μs), in an effort to outpace any significant temperature increase of the inner wall, which would strongly impact the behavior of the cavity.

III. CW MEASUREMENTS

Cavity A had an unusual appearance after Nb_3Sn coating. One half cell had a matte gray appearance like that shown in Fig. 4, but the other half cell had a shinier appearance, suggesting poor Nb_3Sn coverage. Even after removing the coating with an acid etch, and recoating the cavity in a new orientation, the problem persisted on the same half cell, indicating that the niobium material in the half cell might be problematic for the coating process. A Q vs E curve for one of the best performances of the cavity is shown in Fig. 7. Temperature maps confirmed that the high residual resistance R_{res} is primarily caused by the half cell with the unusual appearance [25]. However, the 4.2 K curve still shows significantly higher Q than a niobium cavity would have, indicating that the Nb_3Sn coating strongly improves the cavity's performance.

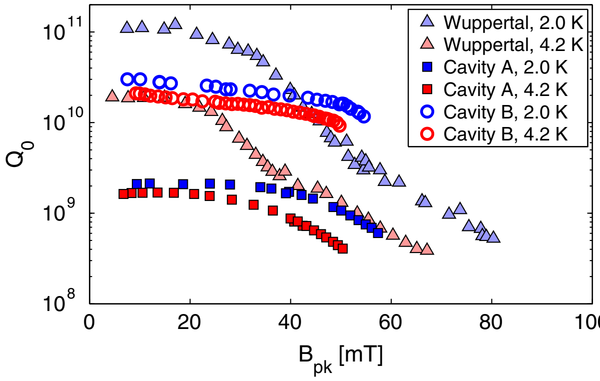

FIG. 7. RF performance curve of cavities A and B compared to the Wuppertal cavity from Fig. 2. Cavity A's high R_{res} appears to be caused by problems with the niobium substrate. Cavity B does not exhibit the strong Q-degradation observed in the other cavities. Uncertainty in Q and E is approximately 10%.

Another prominent feature of the performance curves is a Q-slope which is very similar to that observed by Wuppertal in Fig. 2.

Both half cells of cavity B had a matte gray appearance, indicating good Nb_3Sn coverage. Q vs E of this cavity can also be seen in Fig. 7. Unlike previous low frequency Nb_3Sn cavities, it does not show a strong reduction in Q_0 above ~30–40 mT. At 4.2 K, at medium fields, the Q_0 is up to approximately 10 times higher than that of the Wuppertal cavity, and approximately 20 times higher than a niobium cavity. At 2 K, the Q_0 is only slightly higher than at 4.2 K, indicating that residual resistance dominates over BCS, with R_{res} value of ~9 nΩ, similar to most Wuppertal cavities [11]. However, high Q_0 values persist to larger B_{pk} values than for the very low R_{res} Wuppertal cavity in the figure.

Quench occurred at approximately 55 mT at 2 K (corresponding to an accelerating field of ~13 MV/m), which was preceded by a sharp drop in Q_0 on the order of 10%, as well as preheating on the temperature map. The preheating was highly localized, as shown in Fig. 8. After quench, the same area showed further increased heating, which is consistent with this being the quench location: locally the temperature spikes to near or above T_c during quench, then cools rapidly back to the helium temperature, trapping lossy flux due to thermocurrents. Our observations suggest that the limitation is a defect that becomes normal conducting when the Q_0 drop occurs, and triggers thermal breakdown at slightly higher fields. The dominance of this spot on the temperature map shows that this is a local problem—a defect—not a global problem with Nb_3Sn. Furthermore, though it was accompanied by a large decrease in Q_0, the Wuppertal cavity reached significantly higher CW fields than cavity B, so the limitation cannot be attributed to a fundamental problem with Nb_3Sn.

Q_0 was measured as a function of temperature, as shown in Fig. 9. There was no sign of Q_0 change near the T_c of niobium, 9.2 K, indicating excellent Nb_3Sn coverage of the surface. The high-temperature range is highlighted in the inset, from which a T_c of 18.0 ± 0.1 K is measured. Q_0 was converted to a weighted average surface resistance via $R_s = G/Q_0$. In addition, frequency data measured using a network analyzer as a function of temperature was converted to penetration depth. A combined fit of these two data sets was performed using a polymorphic BCS analysis [26]. The fit is shown in Fig. 10.

Table I lists the material parameters obtained from the $R_s(T)$ fit, together with additional parameters calculated

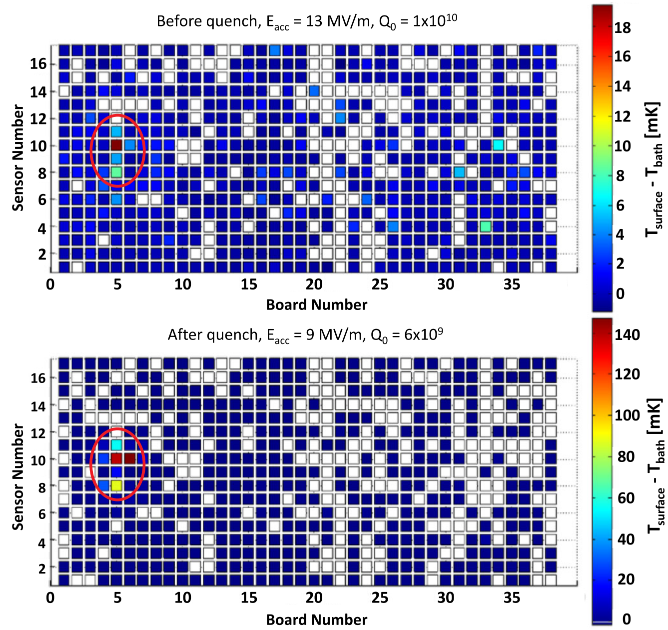

FIG. 8. Temperature maps of cavity B before quench, close to the quench field (top) and after the first quench (bottom). Broken resistors are given a white color. The region of strong localized heating is circled. Note the difference in scale between the top and bottom.

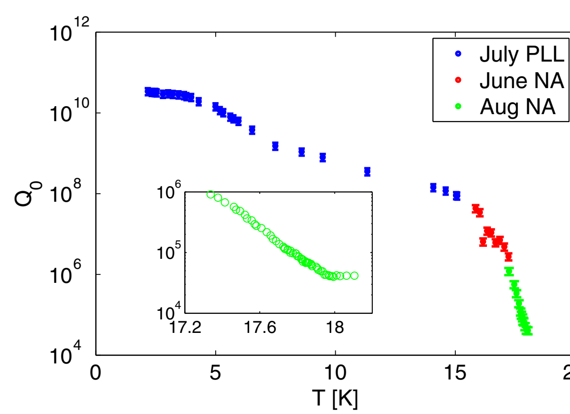

FIG. 9. Q vs T of the cavity B measured with phase lock loop (PLL) or with network analyzer (NA) with weak coupling such that the $Q_0 \sim Q_L$ (left); R_s vs T of cavity B from PLL data and polymorphic BCS fit (right).

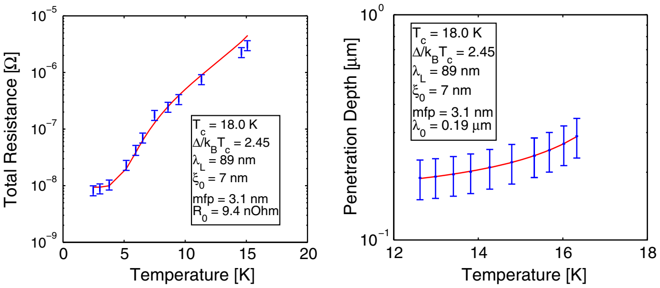

FIG. 10. R_s vs T (left) and λ vs T (right) of cavity B and combined polymorphic BCS fit.

using Ginzburg-Landau theory. These parameters agree well with published data [27,28]. Figure 11 compares B_{c1} to the R_s vs B data, showing that the cavity far exceeds B_{c1} without a significant increase in surface resistance.

IV. PULSED MEASUREMENTS

A typical pulse at 4.2 K is shown in Fig. 12. With the rf input coupler set to $Q_{\mathrm{ext}} = 2 \times 10^6$, cavity B quenches in $\sim$60 μs, reaching $B_{pk} \sim 100$ mT. This is nearly twice the maximum field achieved in CW measurements.

Figure 13 shows the effect of decreasing the forward power on the quench field at 4.2 K. As the klystron power decreases, it takes longer for the cavity to quench, and the quench field decreases due to thermal effects (heating of the inner cavity wall by the rf fields). If the cavity were reaching a fundamental magnetic field limit, then the pulse length should not matter—the cavity should always quench at the same field at a given temperature. Our interpretation is that as the cavity fills with rf energy, the temperature of

TABLE I. Measured and calculated properties of the Nb_3Sn film produced by preparation B.[a]

Property	Value	Derivation
$\lambda_L(0)$ [nm]	89 ± 9	[29], 10% uncertainty assumed
$\xi_0(0)$ [nm]	7.0 ± 0.7	[29], 10% uncertainty assumed
T_c [K]	18.0 ± 0.1	observed from Q vs T
Δ/k_bT_c	2.5 ± 0.2	fit to Q vs T
l [nm]	3 ± 1	fit to Q vs T
R_{res} [nΩ]	9 ± 2	fit to Q vs T
$\lambda_{\mathrm{eff}}(0)$ [nm]	160 ± 20	$\lambda_L\sqrt{1+\frac{\xi_0}{l}}$ [30]
$\xi_{GL}(0)$ [nm]	3.0 ± 0.4	$0.739[\xi_0^{-2}+\frac{0.882}{\xi_0 l}]^{-1/2}$ [31]
κ	54 ± 11	$\lambda_{\mathrm{eff}}/\xi_{GL}$ [30]
$B_c(0)$ [T]	0.47 ± 0.09	$\frac{\phi_0}{2\sqrt{2}\pi\lambda_{\mathrm{eff}}\xi_{GL}}$ [30]
$B_{c1}(0)$ [T]	0.025 ± 0.007	$B_c\frac{\ln\kappa}{\sqrt{2}\kappa}$ [30]
$B_{sh}(0)$ [T]	0.39 ± 0.08	$B_c(\frac{\sqrt{20}}{6}+\frac{0.5448}{\sqrt{\kappa}})$ [32]

[a]For calculations of critical fields from material parameters, Ginzburg Landau theory is applied outside its validity, so there will be corrections on the order of a few percent to the low-temperature critical fields.

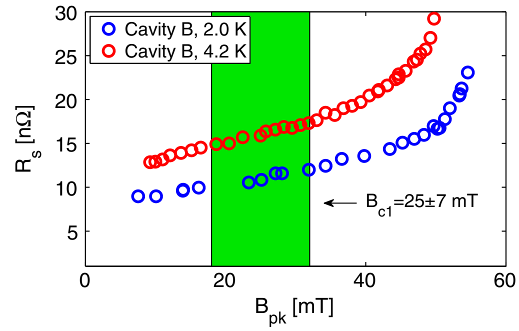

FIG. 11. R_s vs B curves of cavity B compared to the measured B_{c1}, which the cavity clearly exceeds without a significant increase in R_s.

the inner wall of the cavity T_w becomes noticeably higher than the ambient temperature T, and quench occurs at $B_{sh}(T_w)$, which is significantly smaller than $B_{sh}(T)$. Assuming that the cavity quenches due to heating, a very simple thermal model was introduced and applied to the data with a one-parameter fit. It agrees well with the trend, supporting the conclusion that even with 1 MW of power, the cavity is not filling with rf energy fast enough to fully circumvent thermal effects.

This measurement was repeated in helium gas, at constant forward power (as high as possible), at ambient temperatures T up to T_c. The method from [33] was used to extract the quench field, determined by when the Q_0 had dropped to a value corresponding to 90% of the cavity still being superconducting. The result is shown in the Fig. 14, along with $B_{sh}(T)$ and $B_{c1}(T)$ from parameters in Table I. Results from measurements by Hays [33] and Campisi [34] on Nb_3Sn cavities are also shown.

Close to T_c, above $\sim$16 K, where $B_{sh}(T)$ is relatively small, B_{quench} follows the expected $1-(\frac{T}{T_c})^2$ dependence, and indeed it approaches the superheating field. This is expected, as $B_{sh}(T)$ is the surface magnetic field at which flux is predicted to penetrate for an ideal surface at temperature T. The difference between $B_{\mathrm{quench}}(T)$ and

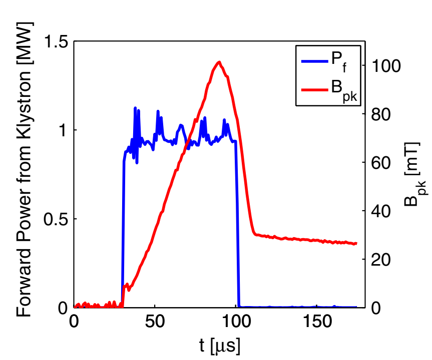

FIG. 12. Nominally square forward power klystron pulse at 4.2 K and cavity response field B_{pk} measured from transmitted power signal.

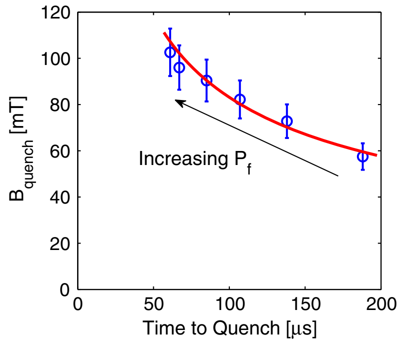

FIG. 13. Reducing the forward power from the klystron increases the time to quench and decreases the quench field. The red curve is a one-parameter fit to the data based on a simple thermal model.

$B_{sh}(T)$ is likely due to some combination of the following effects: (i) heating from rf (surface resistance is quite large at these temperatures) (ii) reduction in the energy barrier to flux penetration caused by surface defects with size on the order of the coherence length, and (iii) magnetic field enhancement at sharp edges [35,36].

At low temperatures, the quench field is lower than the theoretical limit set by the superheating field, but in Fig. 13, we see that near 4.2 K, it depends on the forward power, and insufficient power was available to reach a fundamentally limiting surface magnetic field before thermal effects cause quench.

At all temperatures, the quench field measured in this study is far higher than B_{c1}, further proving that it is not a fundamental limit.

At high temperatures, the plot of cavity B closely resembles those of Campisi and Hays, and all seem to follow B_{sh}. However, at lower temperatures, the data of these three plots are smaller than the predicted B_{sh}. This behavior is similar to measurements of niobium cavities affected by high field Q-slope (HFQS). With the standard treatment to avoid HFQS of EP/120 °C bake, fields close to $B_{sh}^{Nb} \sim 200$ mT are observed, but without this treatment, pulsed measurements are limited to ∼100–150 mT [33,34,37]. This shows that a deviation of the pulsed quench field from B_{sh}, like we see with Nb_3Sn, can be caused by a curable thermal overheating mechanism. It is also possible that the deviation could be caused by nucleation of flux penetration on surface defects. In this case, there is experimental data to suggest that a mechanism such as the vortex line nucleation model would describe the field limit [38–41].

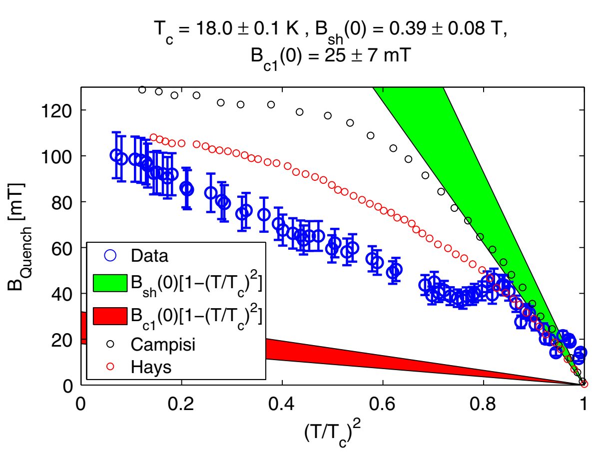

FIG. 14. Quench field as a function of temperature at constant P_f.

V. DISCUSSION

It is not immediately obvious why an extra long annealing step would cause cavity B to have much less severe Q-slope than cavities prepared with the Wuppertal recipe. One explanation might be that there is something special about Cornell's coating method, that the chamber is especially clean, or that the temperatures or times are different in a beneficial way. Interestingly, cavity A was prepared in the same chamber with approximately the same procedure as cavity B except for the extra long anneal, and it exhibits a Q-slope that is similar to that observed in the Wuppertal cavities. The fact that the losses at a given field are similar suggests that the mechanism is the same as that from the Wuppertal cavities, which would mean that without the additional annealing time, there is nothing special about Cornell's coating method that prevents strong Q-slope. But it is also plausible that the Q-slope in cavity A results from a different mechanism caused by the unusually high R_{res} spots.

One obvious change in the material brought about by the extra annealing time is the increase in grain size visible in Fig. 6. If the grain boundaries were acting as weak links, where losses occur as current passes through them, then one would expect that having fewer boundaries would result in smaller losses. A simple model of grain boundary dissipation in superconductors under strong rf fields gives a field dependant surface resistance of $R_s = \frac{\alpha B \Delta}{e a^3 \mu_0}$, where a is the grain size, Δ is the superconducting gap, and α is a fit parameter describing the distribution of electrical properties of grain boundaries [42]. The linear dependence of R_s on B predicted by this model is exhibited by cavity B below the onset of strong defect heating, as shown in Fig. 11. In addition, the size of the Nb_3Sn grains in cavity B was approximately twice that of those in cavity A, and it has a correspondingly smaller R_s, as predicted by this model. This suggests that weak link behavior might be the cause of losses above what is expected from BCS resistance in these Nb_3Sn cavities.

An annealing step after removing the tin source was investigated by researchers at Siemens. At these temperatures, atomic transport for the growth of the Nb_3Sn layer is largely accomplished by diffusion of tin through the grain boundaries [43], which can lead to compounds between grains with undesirable stoichiometry. With the addition of the annealing step, Siemens researchers hoped to prevent the formation of off-stoichiometric compounds that can act as weak links between grains. They observed a "cleaning" and strengthening of the grain boundaries—they found that when subjected to mechanical stress, cracking in the layer shifted from intergranular to intragranular—but found that there was no improvement in the microwave performance [14]. However, unlike the Wuppertal cavities, the Siemens cavities were not afflicted with strong Q-slope. One possible explanation is that unlike the Wuppertal cavities, which were coated with the tin source heated to ~1200 °C and the cavity at ~1100 °C, the Siemens cavities were coated with the tin source and the cavity both at ~1050 °C [14]. If the Siemens procedure resulted in grain boundaries that were satisfactorily clean immediately after coating not to produce weak links, then an additional anneal may not have improved performance. However, after using the Wuppertal recipe, preparation B's additional anneal with a lower tin vapor pressure—in addition to increasing grain size—may help to improve stoichiometry in the grain boundaries, reducing the weak-link behavior, and leading to smaller losses.

It should be mentioned that Wuppertal researchers also attempted a long annealing step (in addition to their standard 30 minute anneal to remove excess tin from the surface). In hopes of increasing the size of the Nb_3Sn grains, they annealed at 1250 °C for 24 hours. These preliminary studies produced an average grain size of 5 μm, but they also caused enhanced diffusion of tin into grain boundaries [11].

If the results of preparation B are repeatable, then the focus of Nb_3Sn SRF research can shift from avoiding Q-slope to reaching higher fields before quench. Siemens researchers found that the data for the maximum field reached by their cavities was normally distributed, leading them to conclude that random defects limited the performance of their cavities. Similarly, in this study, temperature maps showed that cavity B was defect limited. This suggests that the next step should be to find preparation methods that avoid defects that restrict B_{pk} far below B_{sh}, which—as indicated by pulsed measurements—should be the ultimate limit. At Cornell, plans are in place to study electropolishing for smoother substrate surfaces, and ways to decrease the number of grain boundaries, which could act as both weak links and as defects.

There are other issues that should be addressed in the longer term. The thermal conductivity of Nb_3Sn at a given temperature is significantly smaller than that of Nb, so thermal instability is a concern as more power is deposited in the walls at high fields. However, because the Siemens TE cavities reached fields higher than 100 mT at 10 GHz where R_{BCS} is high, it should not be a concern up to similar fields in a 1.3 GHz cavity with minimal Q-slope. R_{res} should also be studied, to try to reproducibly achieve the small level of the Wuppertal cavity in Fig. 2. However, if particle accelerator cavities could be produced that reach 100 mT with the R_{res} of cavity B and minimal Q-slope at 4.2 K, they would be beneficial for a wide variety of applications.

VI. CONCLUSIONS

Surface magnetic fields up to ~55 mT, far above $B_{c1} = 25 \pm 7$ were measured in a 1.3 GHz single cell Nb_3Sn SRF cavity, without the strong Q-slope that had been observed in previous cavities. The cavity was treated with an alternative preparation from previous cavities of its type, and a speculative explanation for the improvement was proposed, based on weak links at grain boundaries. The maximum field was quench limited at a defect, and there is no indication of any fundamental mechanism that would prevent future Nb_3Sn cavities from reaching even higher fields. In pulsed measurements, fields were reached approximately twice as high as those in CW measurements, demonstrating the great potential of this material. Future research on preparation methods to achieve better Nb_3Sn surfaces can be expected to overcome nonfundamental limitations as they have in niobium. Roughly extrapolating the trend in B_{quench} from the high temperature data down to 4.2 K yields a predicted quench field well above even $B_{sh}^{\mathrm{Nb}} = 200$ mT for a Nb_3Sn cavity free of nonfundamental limitations. Even with the current performance achieved, Nb_3Sn now becomes a promising alternative material for certain future accelerators, as at usable accelerating fields ~12 MV/m, we have shown that at 4.2 K Nb_3Sn cavities can achieve a Q_0 of 10^{10}, ~20 times higher than niobium.

ACKNOWLEDGEMENTS

Work supported by NSF Career Grant No. PHY-0841213, DOE award No. ER41628, and the Alfred P. Sloan Foundation. This work made use of the Cornell Center for Materials Research Shared Facilities which are supported through the NSF MRSEC program (DMR-1120296). The authors would like to express special thanks to summer student F. Wohlfarth for assistance in cavity preparation; to M. Thomas for help with surface analysis; to N. Valles for writing BCS polymorphic fit program; to J. Halbritter, author of the SRIMP program for calculating R_s and λ; to P. Kneisel for excellent summary notes of the history of Nb_3Sn SRF research [43]; and to H. Padamsee for helpful discussions.

[1] J. Matricon and D. Saint-James, Phys. Lett. **24A**, 241 (1967).

[2] M. Liepe, in *Proceedings of the Third Workshop on Energy Recovery Linacs, Ithaca, 2009.*

[3] T. Powers, in *Proceedings of the Sixteenth Conference on RF Superconductivity, Paris, 2013*, edited by C. Antoine, S. Bousson, and G. Martinet (JACoW, Paris, 2013).
[4] The large thermodynamic critical field $B_c = \frac{\phi_0}{2\sqrt{2}\pi\lambda_{\mathrm{eff}}\xi_{GL}}$ [5] of Nb_3Sn is a consequence of its relatively small coherence length.
[5] G. Arnolds-Mayer, in *Proceedings of the Second Workshop on RF Superconductivity, Geneva, 1984*.
[6] H. Padamsee, J. Knobloch, and T. Hays, *RF Superconductivity for Accelerators* (Wiley-VCH, New York, 2008), p. 521.
[7] B. Hillenbrand, H. Martens, H. Pfister, K. Schnitzke, and Y. Uzel, IEEE Trans. Magn. **13**, 491 (1977).
[8] P. Kneisel, O. Stoltz, and J. Halbritter, IEEE Trans. Magn. **15**, 21 (1979).
[9] G. Arnolds and D. Proch, IEEE Trans. Magn. **13**, 500 (1977).
[10] J. Stimmell, Ph.D. thesis, Cornell University, 1978.
[11] G. Müller, P. Kneisel, and D. Mansen, in *Proceedings of the Fifth European Particle Accelerator Conference, Sitges, 1996* (IOP, Sitges, 1996).
[12] G. Arnolds-Mayer and E. Chiaveri, in *Proceedings of The Third Workshop on RF Superconductivity, Chicago, 1986*.
[13] I. E. Campisi and Z. D. Farkas, in *Proceedings of the Second Workshop on RF Superconductivity, Geneva, 1984*.
[14] B. Hillenbrand, in *Proceedings of the First Workshop on RF Superconductivity, Karlsruhe, 1980*.
[15] B. Hillenbrand, N. Krause, H. Pfister, K. Schnitzke, and Y. Uzel, Siemens AG, Technical Report, 1981.
[16] G. Müller, H. Piel, J. Pouryamout, P. Boccard, and P. Kneisel, in *Proceedings of the Workshop on Thin Film Coating Methods for Superconducting Accelerating Cavities, DESY, 2000*, edited by D. Proch (TESLA Report 2000-15, Hamburg, 2000).
[17] P. Boccard, P. Kneisel, G. Müller, J. Pouryamout, and H. Piel, in *Proceedings of the Eighth Workshop on RF Superconductivity, Padova, 1997*.
[18] A. Gurevich, Appl. Phys. Lett. **88**, 012511 (2006).
[19] M. Perpeet, A. Cassinese, M. Hein, T. Kaiser, G. Muller, H. Piel, and J. Pouryamout, IEEE Trans. Appl. Supercond. **9**, 2496 (1999).
[20] S. Posen and M. Liepe, in *Proceedings of the Fifteenth Conference on RF Superconductivity, Chicago, 2011*, pp. 886–889.
[21] M. Peiniger, Ph.D. thesis University of Wuppertal, 1989.
[22] V. Shemelin, in *Proceedings of the Fourteenth Conference on RF Superconductivity, Berlin, 2009*, pp. 528–532.
[23] E. Haebel, A. Mosnier, and J. Sekutowicz, in *Proceedings of the 15th Conference on High Energy Accelerators, Hamburg, 1992*, edited by J. Rossbach (World Scientific, Singapore, 1992), Vol. 2, pp. 957–959.
[24] J. Knobloch, Ph.D. thesis, Cornell University, 1997.
[25] S. Posen, in *European Linear Collider Workshop ECFA LC2013* (Hamburg, 2013).
[26] N. R. Valles, Ph.D. thesis, Cornell University, 2014.
[27] A. Godeke, Supercond. Sci. Technol. **19**, R68 (2006).
[28] M. Hein, M. Perpeet, and G. Muller, IEEE Trans. Appl. Supercond. **11**, 3434 (2001).
[29] M. Hein, *High-Temperature-Superconductor Thin Films at Microwave Frequencies* (Springer, New York, 1999).
[30] M. Tinkham, *Introduction to Superconductivity* (Dover Publications, New York, 2004), p. 454.
[31] T. P. Orlando, E. J. McNiff, S. Foner, and M. R. Beasley, Phys. Rev. B **19**, 4545 (1979).
[32] M. K. Transtrum, G. Catelani, and J. P. Sethna, Phys. Rev. B **83**, 094505 (2011).
[33] T. Hays, H. Padamsee, and N. Studies, in *Proceedings of the Eighth Workshop on RF Superconductivity, Padova, 1997*, pp. 789–794.
[34] I. Campisi, IEEE Trans. Magn. **21**, 134 (1985).
[35] J. Knobloch, R. Geng, M. Liepe, and H. Padamsee, in *Proceedings of the Ninth Workshop on RF Superconductivity, 1999*, p. 77.
[36] H. Tian, G. Ribeill, C. Xu, C. E. Reece, and M. J. Kelley, Appl. Surf. Sci. **257**, 4781 (2011).
[37] N. Valles and M. Liepe, in *Proceedings of the Fifteenth Conference on RF Superconductivity, Chicago, 2011*, p. 4.
[38] G. Catelani and J. P. Sethna, Phys. Rev. B **78**, 224509 (2008).
[39] T. Yogi, G. J. Dick, and J. E. Mercereau, Phys. Rev. Lett. **39**, 826 (1977).
[40] K. Saito, in *Proceedings of the Eleventh Workshop on RF Superconductivity, DESY, 2003*, p. 1.
[41] T. Junginger, Ph.D. thesis, Ruperto-Carola University of Heidelberg, 2012.
[42] B. Bonin and H. Safa, Supercond. Sci. Technol. **257**, 257 (1991).
[43] P. Kneisel, Jefferson Lab Technical Report, 2012.